# Dynamics of Localized Structures in Vectorial Waves

Emilio Hernández-García, Miguel Hoyuelos,* Pere Colet, and Maxi San Miguel
*Instituto Mediterráneo de Estudios Avanzados, IMEDEA† (CSIC-UIB), Campus Universitat Illes Balears, E-07071 Palma de Mallorca, Spain*
(Received 13 July 1999)

Dynamical properties of topological defects in a two dimensional complex vector field are considered. These objects naturally arise in the study of polarized transverse light waves. Dynamics is modeled by a vector complex Ginzburg-Landau equation with parameter values appropriate for linearly polarized laser emission. Creation and annihilation processes, and self-organization of defects in lattice structures, are described. We find "glassy" configurations dominated by vectorial defects and a melting process associated with topological-charge unbinding.

PACS numbers: 42.65.Sf, 05.45.–a, 47.54.+r

A variety of nonlinearly evolving fields display states consisting of distinct localized objects with some kind of particlelike behavior. Examples are vortices in fluids, superfluids and superconductors, solitary waves in chemical media, and oscillons in granular layers, among others [1]. These localized structures often organize the geometry and the dynamics of the host medium, so that they become "building blocks" of regular patterns and of spatiotemporal chaos [2,3]. In this situation, an understanding of complex evolving configurations can be achieved in terms of the interaction rules of the particlelike entities. An important class of localized objects is *defects* that appear as a consequence of spontaneous symmetry breaking in the surrounding medium. These objects carry topological properties which endorse them with a characteristic stability and robustness. Its presence is ubiquitous both in and out of equilibrium and often mediates nonequilibrium dynamical processes.

Optical cavities containing nonlinear optical materials have been specially prolific in providing examples of localized structures [4]. They can take the form of vortices or bright or dark dissipative spatial solitons. The ability of "writing," "erasing," and moving around these localized light spots opens promising ways of achieving parallel information processing. There is, however, an important property of light that is just becoming to be appreciated in this context: the vector nature of the electromagnetic field. Sometimes, the polarization degree of freedom is fixed by material anisotropies or by experimental arrangements. But, when free to manifest, it leads to striking topological phenomena [5].

A classification of topological singularities in electromagnetic fields propagating paraxially in linear media can be found in [6]. Nonlinear generation and propagation, as occurring in lasers, favors particular polarization states (circular or linear, for instance) which should be taken as the relevant background states on which topological defects may appear in nonlinear systems. Classification of topological defects on such vector nonlinear backgrounds was established in [7], improving on earlier work [8]. While in particular limits some information on isolated defects may be obtained analytically [7], there is a lack of understanding about complex dynamic states. Here we explore these states for general nonconservative and nonrelaxational dynamics. We study which kinds of defects spontaneously emerge and describe their stability, self-organization, and annihilation. Transitions between different spatiotemporal regimes, mediated by defect-behavior changes, are found: A "vectorial defect" can entrain the whole system and dominate "frozen" configurations whereas topological-charge unbinding leads to the melting of this frozen phase into a new dynamical regime.

Our study is made in the context of a spatially two dimensional model appropriate for laser emission from wide-aperture resonators, the vector complex Ginzburg-Landau equation (VCGLE) [9]. The VCGLE can describe also, in appropriate ranges of parameters, other kinds of systems such as two-component Bose condensates [10] and counterpropagating waves in nonlinear media [11]. In general, the VCGLE describes the complex envelope of any oscillating vector field close enough to a homogeneous Hopf bifurcation, which leads to a variety of complex spatiotemporal phenomena. Through this Letter, however, we will restrict the study to parameter ranges of interest in optics.

The VCGLE can be written as

$$\partial_t A_\pm = A_\pm + (1 + i\alpha)\nabla^2 A_\pm - (1 + i\beta)(|A_\pm|^2 + \gamma|A_\mp|^2)A_\pm . \quad (1)$$

$A_\pm$ are the two components of the vector complex field. In optics they are identified with the right and left circularly polarized components of the transverse field. Other forms of this equation can be written [8] in terms of the Cartesian components $(A_x, A_y)$, which are related to the circular ones by $A_x = (A_+ + A_-)/\sqrt{2}$ and $A_y = (A_+ - A_-)/i\sqrt{2}$. When interpreted as a set of two coupled fields the model gives the opportunity to explore synchronization of spatiotemporal chaos [3,12]. The real parameters $\alpha$ and $\beta$ are associated with the strength of nondissipative spatial coupling (optical diffraction) and nonlinear frequency shift (optical detuning), respectively. As for laser systems the condition $1 + \alpha\beta > 0$ is always

 0031-9007/00/85(4)/744(4)$15.00 

satisfied [9]; we will consider only this case. This corresponds to the Benjamin-Feir stable range, where there are stable plane-wave solutions of Eq. (1). The parameter $\gamma$ (a real number in lasers) represents the coupling between the polarization components. We consider a weak coupling situation ($\gamma < 1$) so that stable uniform solutions satisfy $|A_+| = |A_-|$. This corresponds to a laser emitting linearly polarized light.

For $\gamma = 0$ Eq. (1) becomes a pair of independent scalar complex Ginzburg-Landau equations (CGLE). A localized structure which appears in characteristic configurations of the two dimensional CGLE [13] is a topological defect: a "vortex" where the amplitude is exactly zero and thus the phase of the field is not defined. In the regime where plane waves are stable, a spiral wave develops around the defect. It behaves asymptotically as a traveling wave (TW) of a particular wave number dynamically selected by the defect [14].

When $\gamma \neq 0$ the two components $A_+$ and $A_-$ become coupled and we have genuine vector effects. The classification of defects of the vector field in [7] was elaborated in terms of the Cartesian components of the field $(A_x, A_y)$, but it is better for our purposes to recast it in terms of the circular components $A_\pm = |A_\pm| e^{i\phi_\pm}$: Eq. (1) admits a continuous family of TW solutions for $A_+$ and $A_-$ which are the obvious generalizations to $d = 2$ of the one dimensional solutions described in [9]. Defects appear when different solutions of this family are selected in different regions of the space. The different solutions can be matched continuously except at one point, the defect, where the field has to take a value outside the family. In our case localized zeros in $|A_\pm|$ are defects. Two topological charges $n_\pm$ associated with each defect are defined by $2\pi n_\pm \equiv \oint d\vec{r} \cdot \vec{\nabla}\phi_\pm$, where the integral is around a closed path encircling the defect. We find the following defects in our dynamical system: A *vectorial defect* is a zero in both components of the field at the same point. It is of the *argument* type when $n_+ = n_-$. The background solutions matched around it are TW with the same wave vector for $A_\pm$. A simple *ansatz* for this solution reveals that it selects asymptotically the same wave number as for $\gamma = 0$. If $n_+ = -n_-$ the vectorial defect is of the *director* type and the background solutions are TW for $A_\pm$, again with the same asymptotic wave number, but with different wave vector orientation. Finally, we call *scalar defect* a zero in just one of the two circular field components. The background solutions are TW. The wave number in the component containing the zero decreases with $\gamma$, being the one in the other component always vanishing. Numerically, we do not find defects with $|n_\pm| > 1$. A variety of defect interaction processes are possible which respect the necessary requirement of topological-charge conservation. We now describe some of these processes that occur in our dynamical model.

We first consider [15] the spontaneous formation of defects starting from random initial conditions around the unstable solution $A_+ = A_- = 0$. For short times the dynamics creates a high density of scalar defects. Those of opposite charge in the same component of the field may collide and annihilate in pairs during this transient. At a later stage, and for $\gamma$ not too large, vectorial defects are formed due to the coalescence of two scalar defects, belonging to different field components, which form a bound structure. This later stage is reached later as $\gamma$ becomes smaller. Of course, for $\gamma = 0$ the lack of coupling between the components precludes the formation of vectorial defects. Close to the potential limit $\alpha = \beta$ [16] (which includes the real-coefficient case $\alpha = \beta = 0$) they are neither formed. The appearance of vectorial defects has a strong influence on the dynamics: spiral waves develop around the core in each component which immediately expel out all the scalar defects. Thus the vectorial defects become the organizing centers of the final field configurations (see Fig. 1). The rotation sense of the spiral in each component is determined by the sign of the corresponding topological charge (see figure caption). The long-time configurations are characterized by a structure of cellular domains with nearly constant modulus separated by shocks between the waves. These "frozen" or "glassy" configurations with an extremely slow evolution of the modulus of the field components look similar to configurations found in the scalar CGLE. However, these configurations arise here from the dynamical dominance of the vectorial defects, behaving toward the scalar ones more passively. In the scalar CGLE the difference between the dominant defects and the ones at the domain borders seems to arise from spontaneous amplification of inhomogeneities [17,18]. Here no vectorial defect is

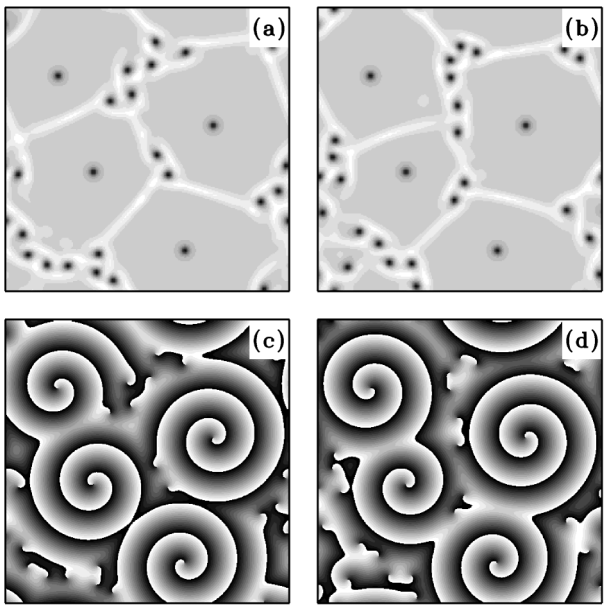


FIG. 1. Long-time field configurations for $\gamma = 0.1$, $\alpha = 0.2$, and $\beta = 2$. (a) $|A_+|^2$, (b) $|A_-|^2$, (c) $\phi_+$, and (d) $\phi_-$. In (c) and (d), the upper-left and lower-right spirals have the same sense, thus identifying its core as an argument defect; the other spirals wind in opposite senses (director defects).

found at the domain borders. The polarization state in the domain around an argument defect is one of constant linear polarization, with direction determined by the phase difference between the spirals. The state around a director defect is also linearly polarized, but with polarization direction rotating around the defect core. Scalar defects do not present a developed spiral wave around them in the situation just described, although it may appear in the charged component when initial conditions producing well-separated scalar defects are used. Its core is circularly polarized.

The frozen configurations occur for relatively small $\gamma$. Increasing $\gamma$ vectorial defects become unstable and they are destroyed leading to a "melting" of the glass phase. We have identified two destruction mechanisms: (i) background instability: one of the two charges forming a vectorial defect is annihilated by an external scalar defect; as a result a free scalar defect is left in the other component of the field and (ii) core instability: the vectorial defect splits in two scalar defects.

The region in parameter space $\alpha$-$\beta$ where process (i) is observed corresponds approximately to the region where for the scalar CGLE the phase spirals are convectively unstable [19]. The spirals remain in place and look stable because perturbations are effectively ejected away because of the group velocity on the spiral wave. As $\gamma$ is increased from zero the stability of the spirals is modified: At a given value of $\gamma$, the group velocity is not strong enough to overwhelm the growth of the perturbations, the spirals becoming absolutely unstable. At this point the domains around the vectorial defects are uneffective as exclusion zones, so that scalar defects previously confined to the domain border can approach the vectorial defect core (Fig. 2). This allows for mechanism (i) to take place. Although this picture is valid for both kinds of vectorial defects, director defects survive for larger $\gamma$ than argument ones. For the parameter values of Fig. 1, argument defects become unstable at $\gamma \simeq 0.3$, while director defects remain stable up to $\gamma \simeq 0.35$. For larger $\gamma$ only scalar defects are found numerically. The different stability range of argument and director defects can be understood through a linear stability analysis of the vector spirals focusing in its far-field plane-wave structure. An extension of the $d = 1$ analysis [9] indicates that as $\gamma$ is increased polarization phase instabilities are such that corotating spirals (the background solutions for argument defects) become *convectively* unstable before counterrotating spirals associated with director defects. The calculation of the absolute instability limit is quite involved, but the result for the convective instability suggests that corotating spirals become absolutely unstable before counterrotating ones.

Process (ii) is roughly present in the region of parameter space $\alpha$-$\beta$ where the spirals are stable in the scalar case. The splitting of a director defect is shown in Fig. 3. The size of the vectorial defect core is much smaller than the size of the core of the two scalar defects that remain at the end of the process. Also in this case argument defects become unstable for smaller $\gamma$ than director defects. For example, for the parameter values of Fig. 3 argument defects already split for $\gamma = 0.75$. The splitting mechanism has been previously described in Ref. [7] for the real-coefficient case ($\alpha = \beta = 0$), where a greater symmetry between director and argument defects seems to be present. More in general, approaching the line $\alpha = \beta$, we observe numerically that director and argument defects of initial configurations such as the one in Fig. 1 split spontaneously, even for very small values of $\gamma$.

For $\gamma$ high enough, the vectorial defects always disappear following one of the two mechanisms described above. The system then presents a faster disordered dynamics (a kind of *gaslike* phase) dominated by the scalar defects, which are conserved in number during very long times. A typical snapshot is shown in Fig. 4. At the defect core one of the components vanishes, and the modulus of the other has a local maximum. Thus the localized objects are circularly polarized and impose some elliptic polarization to their neighborhood. The spiral wavelength around scalar defects increases with $\gamma$, so that well-developed spirals do not fit in the domains for $\gamma$ close to one. Domains are thus less effective as exclusion zones and defects more mobile. The vortex unbinding transition between the glassy and the gaslike phases can be described quantitatively in terms of entropy and mutual information measures [12,20].

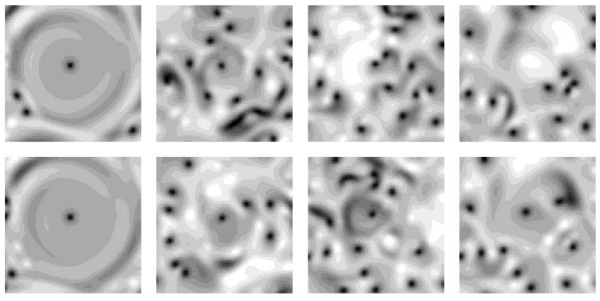

FIG. 2. Annihilation of a director defect ($\gamma = 0.35$, $\alpha = 0.2$, $\beta = 2$). Upper row: $|A_+|^2$, lower row: $|A_-|^2$. From left to right: $t = 90, 190, 270, 290$. The initial condition was the configuration of Fig. 1. Only a part of the simulation domain is shown.

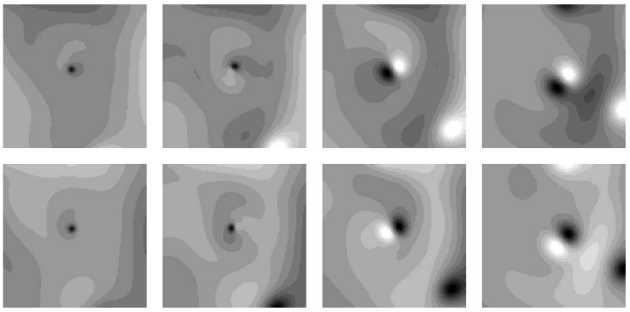

FIG. 3. Splitting of a director defect ($\alpha = 0.7$, $\beta = 2$, $\gamma = 0.95$). Upper row: $|A_+|^2$; lower row: $|A_-|^2$. From left to right: $t = 50, 100, 150, 200$. The initial state formed spontaneously under $\gamma = 0.9$.

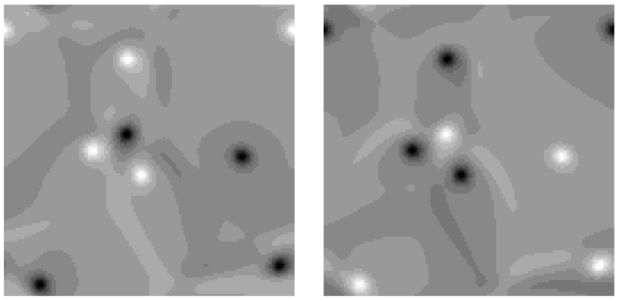

FIG. 4. An evolving gaslike state, dominated by scalar defects ($\alpha = 0.2$, $\beta = 2$, $\gamma = 0.8$). Left: $|A_+|^2$; right: $|A_-|^2$.

We finally discuss the emergence of self-organized ordered structures of defects. In the dynamics leading to configurations as the one in Fig. 1 there are cases, particularly for small $\gamma$, in which only one or a few vectorial defects are formed. They immediately push the scalar defects out of the limits of their large domains, so that a large number of scalar defects are compressed in a limited region of space. In this situation the "gas" of scalar defects "crystallizes" forming a stable square lattice with alternating positive and negative charges as in an ionic crystal (see Fig. 5). The lattice in one of the components fills the interstitials of the other. Once the lattice is formed, the vectorial character of the field is no longer required to keep the lattice stable. In fact, crystalline aggregation of defects was previously observed in the scalar CGLE in special situations (when $\alpha$ is close to $\beta$; see [17]). In that case, however, very special initial conditions are needed to obtain the lattice, whereas here the vectorial defect creates a large exclusion island which compresses the scalar defects and leads to the spontaneous condensation, in rather general conditions, of a highly dense crystal.

In summary, we have described phenomena associated with defect dynamics in vector nonlinear media. Crystal-, gas-, and glasslike phases are found with transitions between them mediated by processes in which the vector nature of the field and the defects plays an important role. Optical active media are the natural systems in which to search for experimental realizations of these phenomena. In addition to applications to information storage and processing, the particlelike objects studied here present spatial localization of both light intensity and optical polarization. This makes them very interesting from the point of view of applications leading to atom trapping and cooling.

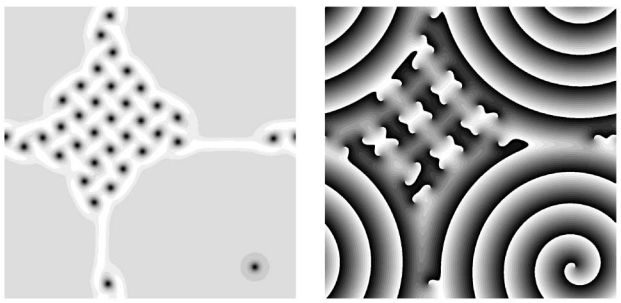

FIG. 5. Crystal of defects, compressed by the vectorial defect in the lower-right corner ($\alpha = 0.2$, $\beta = 2$, $\gamma = 0.01$). Condensation occurred spontaneously starting from random initial conditions. Left: $|A_+|^2$; right: $\phi_+$.

Financial support from DGICYT (Spain, Projects No. PB94-1167 and No. PB97-0141-C02-02) and from the European Commission (TMR Project No. QSTRUCT FMRX-CT96-0077) is acknowledged. M. H. also acknowledges support from FOMEC Project No. 290, Departamento de Física FCEyN, UNMP, and from CONICET Grant PIP No. 4342.

*Present address: Departamento de Física FCEyN, Universidad Nacional de Mar del Plata, Mar del Plata, Argentina.
†http://www.imedea.uib.es/PhysDept/

[1] H. Riecke, in *Pattern Formation in Continuous and Coupled Systems,* edited by M. Golubitsky, D. Luss, and S. H. Strogatz (Springer, New York, 1999); L. M. Pismen, *Vortices in Nonlinear Fields* (Oxford University Press, New York, 1999).
[2] M. van Hecke, Phys. Rev. Lett. **80**, 1896 (1998).
[3] A. Amengual *et al.,* Phys. Rev. Lett. **78**, 4379 (1997).
[4] F. T. Arecchi *et al.,* Phys. Rev. Lett. **67**, 3749 (1991); C. O. Weiss *et al.,* Appl. Phys. B **68**, 151 (1999); N. N. Rosanov, in *Progress in Optics,* edited by E. Wolf (North-Holland, Amsterdam, 1996), Vol. 35; M. Brambilla *et al.,* Phys. Rev. Lett. **79**, 2042 (1997); M. Tlidi, P. Mandel, and R. Lefever, Phys. Rev. Lett. **73**, 640 (1994); W. Firth and A. J. Scroggie, Phys. Rev. Lett. **76**, 1623 (1996); C. Etrich, U. Peschel, and F. Lederer, Phys. Rev. Lett. **79**, 2454 (1997); K. Staliunas and V. J. Sánchez-Morcillo, Phys. Rev. A **57**, 1454 (1998); G. L. Oppo, A. J. Scroggie, and W. J. Firth, J. Opt. B **1**, 133 (1999).
[5] R. Bhandari, Phys. Rep. **281**, 1 (1997).
[6] J. V. Hajnal, Proc. R. Soc. London A **414**, 433 (1987); **414**, 447 (1987).
[7] L. M. Pismen, Phys. Rev. Lett. **72**, 2557 (1994); Physica (Amsterdam) **73D**, 244 (1994).
[8] L. Gil, Phys. Rev. Lett. **70**, 162 (1993).
[9] M. San Miguel, Phys. Rev. Lett. **75**, 425 (1995).
[10] R. Graham and D. Walls, Phys. Rev. A **57**, 484 (1998).
[11] M. van Hecke, C. Storm, and W. van Saarloos, Physica (Amsterdam) **134D**, 1 (1999).
[12] E. Hernández-García *et al.,* Int. J. Bifurcation Chaos Appl. Sci. Eng. **9**, 2257 (1999).
[13] H. Chaté and P. Manneville, Physica (Amsterdam) **224A**, 348 (1996).
[14] P. S. Hagan, SIAM J. Appl. Math. **42**, 762 (1982).
[15] We use a numerical pseudospectral method with second order accuracy in time [20] in lattices of size $128 \times 128$. The spatial and temporal discretizations were $\Delta x = 1$, and $\Delta t = 0.05$.
[16] R. Montagne *et al.,* Physica (Amsterdam) **96D**, 47 (1996).
[17] I. S. Aranson, L. Kramer, and A. Weber, Phys. Rev. E **47**, 3231 (1993); **48**, R9 (1993).
[18] M. Hendrey *et al.,* Phys. Rev. Lett. **82**, 859 (1999).
[19] I. S. Aranson *et al.,* Phys. Rev. A **46**, R2992 (1992).
[20] M. Hoyuelos *et al.,* Comput. Phys. Commun. **121–122**, 414 (1999).